

## Additive fungal interactions drive biocontrol of Fusarium wilt disease

New Phytologist

Tao, Chengyuan; Wang, Zhe; Liu, Shanshan; Lv, Nana; Deng, Xuhui et al

<https://doi.org/10.1111/nph.18793>

This publication is made publicly available in the institutional repository of Wageningen University and Research, under the terms of article 25fa of the Dutch Copyright Act, also known as the Amendment Taverne. This has been done with explicit consent by the author.

Article 25fa states that the author of a short scientific work funded either wholly or partially by Dutch public funds is entitled to make that work publicly available for no consideration following a reasonable period of time after the work was first published, provided that clear reference is made to the source of the first publication of the work.

This publication is distributed under The Association of Universities in the Netherlands (VSNU) 'Article 25fa implementation' project. In this project research outputs of researchers employed by Dutch Universities that comply with the legal requirements of Article 25fa of the Dutch Copyright Act are distributed online and free of cost or other barriers in institutional repositories. Research outputs are distributed six months after their first online publication in the original published version and with proper attribution to the source of the original publication.

You are permitted to download and use the publication for personal purposes. All rights remain with the author(s) and / or copyright owner(s) of this work. Any use of the publication or parts of it other than authorised under article 25fa of the Dutch Copyright act is prohibited. Wageningen University & Research and the author(s) of this publication shall not be held responsible or liable for any damages resulting from your (re)use of this publication.

For questions regarding the public availability of this publication please contact  
[openscience.library@wur.nl](mailto:openscience.library@wur.nl)

# Additive fungal interactions drive biocontrol of *Fusarium* wilt disease

Chengyuan Tao<sup>1,2</sup> , Zhe Wang<sup>1,2</sup> , Shanshan Liu<sup>1</sup>, Nana Lv<sup>1</sup>, Xuhui Deng<sup>1</sup> , Wu Xiong<sup>1</sup> , Zongzhan Shen<sup>1,2</sup> , Nan Zhang<sup>1</sup> , Stefan Geisen<sup>3,4</sup> , Rong Li<sup>1,2</sup> , Qirong Shen<sup>1</sup>  and George A. Kowalchuk<sup>5</sup> 

<sup>1</sup>Jiangsu Provincial Key Lab of Solid Organic Waste Utilization, The Key Laboratory of Plant Immunity, Jiangsu Collaborative Innovation Center of Solid Organic Wastes, Educational Ministry Engineering Center of Resource-Saving Fertilizers, Nanjing Agricultural University, Nanjing, Jiangsu 210095, China; <sup>2</sup>The Sanya Institute of Nanjing Agricultural University, Sanya, Hainan 572000, China; <sup>3</sup>Department of Terrestrial Ecology, Netherlands Institute for Ecology (NIOO-KNAW), Wageningen 6708 PB, the Netherlands; <sup>4</sup>Laboratory of Nematology, Wageningen University, Wageningen 6700 AA, the Netherlands; <sup>5</sup>Ecology and Biodiversity Group, Department of Biology, Institute of Environmental Biology, Utrecht University, Utrecht 3584 CH, the Netherlands

## Summary

Author for correspondence:

Rong Li

Email: [lirong@njau.edu.cn](mailto:lirong@njau.edu.cn)

Received: 11 August 2022

Accepted: 23 January 2023

New Phytologist (2023)

doi: 10.1111/nph.18793

**Key words:** banana Fusarium wilt, cooperative fungal interactions, soil disease suppression, *Trichoderma*-amended biofertilizer, *Trichoderma*-*Humicola* consortia.

- Host-associated fungi can help protect plants from pathogens, and empirical evidence suggests that such microorganisms can be manipulated by introducing probiotic to increase disease suppression. However, we still generally lack the mechanistic knowledge of what determines the success of probiotic application, hampering the development of reliable disease suppression strategies.
- We conducted a three-season consecutive microcosm experiment in which we amended banana Fusarium wilt disease-conducive soil with *Trichoderma*-amended biofertilizer or lacking this inoculum. High-throughput sequencing was complemented with cultivation-based methods to follow changes in fungal microbiome and explore potential links with plant health.
- *Trichoderma* application increased banana biomass by decreasing disease incidence by up to 72%, and this effect was attributed to changes in fungal microbiome, including the reduction in *Fusarium oxysporum* density and enrichment of pathogen-suppressing fungi (*Humicola*). These changes were accompanied by an expansion in microbial carbon resource utilization potential, features that contribute to disease suppression. We further demonstrated the disease suppression actions of *Trichoderma*-*Humicola* consortia, and results suggest niche overlap with pathogen and induction of plant systemic resistance may be mechanisms driving the observed biocontrol effects.
- Together, we demonstrate that fungal inoculants can modify the composition and functioning of the resident soil fungal microbiome to suppress soilborne disease.

## Introduction

Microbial communities are present in all environments and cover virtually all host surfaces from skin, gut, and mucosa of animals (Grice & Segre, 2011; Costello *et al.*, 2012) to plant roots and leaves (Bai *et al.*, 2015). They function as a first line of defense against invading pathogens (Shin *et al.*, 2011; Berendsen *et al.*, 2012). A disruption of this microbial defense can lead to increases in disease incidence, which is caused by a subset of harmful microbes (Zhang *et al.*, 2017; Lee *et al.*, 2021). Therefore, rehabilitation or augmentation of the natural defense offered by the host-associated microbiome can provide an effective means to control pathogen populations, such as those causing plant diseases (Mueller & Sachs, 2015; Toju *et al.*, 2018).

Microbiome manipulation can enhance agro-ecosystem function, including soilborne disease prevention (Mueller & Sachs, 2015; Kwak *et al.*, 2018). Both the diversity and composition of the soil microbial community have been found to be linked to soil disease suppressiveness (Elsas *et al.*, 2012; Raaijmakers & Mazzola, 2016). High microbial diversity is likely related to the complexity of microbial interactions and therefore enhances the resistance to invading pathogens (Romanuk *et al.*, 2009; Wei *et al.*, 2015). Also, specific taxa of beneficial microorganisms can protect plants against pathogens (Kwak *et al.*, 2018; Lee *et al.*, 2021). However, optimization of plant-microbial partnerships remains a daunting task given the complexity of plant-microorganism and microorganism-microorganism interactions, and the dependence of these interactions on environmental conditions (Sessitsch *et al.*, 2019). Therefore,

better understanding of the interactions between beneficial microbes, pathogens, and the indigenous soil microbiomes is necessary to support more effective disease suppression.

Using plant probiotics for the biocontrol of plant diseases has been proposed as a sustainable approach for pathogen control and combatting soilborne diseases (Kandula *et al.*, 2015; Hu *et al.*, 2021). Synthetic microbiome association studies using plant probiotics have shown that the manipulation of bacterial community diversity (Hu *et al.*, 2016), bacterial resource competition networks (Wei *et al.*, 2015), or bacterial interspecies interactions (Li *et al.*, 2019) can enhance the resistance of resident bacterial communities to pathogen invasion. Although such studies are beginning to reveal the mechanisms involved in bacterial responses in probiotic treatments, far less is known about how fungal communities are impacted by such treatments and how fungal community dynamics impact disease-suppressive capabilities. Recently, there is a growing interest in exploring the roles that fungi play in environmental and host-associated microbiomes (Jiang *et al.*, 2017; Duran *et al.*, 2018; Wagg *et al.*, 2019; Pierce *et al.*, 2021). Despite growing awareness that fungi in particular the fungal interactions have an immense capacity to affect soil ecological functioning, fungi are frequently overlooked in disease-suppressive soil microbiome studies.

In this study, we carried out series of experiments to examine the progressive impact of *Trichoderma guizhouense* NJAU4742 (*Tg*, a well-studied biocontrol agent of *Fusarium* wilt; J. Zhang *et al.*, 2019) amended biofertilizer on the development of disease suppression in a continuous banana monoculture cropping system. We imposed treatments with *Tg* in the presence and absence of sterilized organic fertilizer (SOF), subsequently monitored fungal communities using quantitative PCR and fungal ITS amplicon sequencing, and complemented these molecular approaches with culture-based experiments to test specific fungal interactions with the pathogen. We specifically sought to (1) determine the fate and the disease suppression capability of *Tg* and (2) reveal the role of changes in the resident fungal community and functioning after inoculation of *Tg* in plant disease suppression. We hypothesized that plant disease suppression induced by *Tg* is the combination product of the direct introduction of pathogen inhibition traits and the indirect effects due to the interspecific interactions with resident microbiome.

## Materials and Methods

### Experimental design

To determine *Tg*-induced fungal community manipulation for the protection of banana plant in the *Fusarium* wilt disease soil, we established a series of microcosm experiments for three crop seasons (each crop season lasts 4 months) of banana cultivation. Experimental soil was collected from a field with a 20-yr history of banana monoculture that suffers from serious *Fusarium* wilt disease (60–70%). Microcosm experiments were established in a glasshouse with average temperature of 30°C and humidity of 70% (108°45'E, 18°38'N). Soil was distributed into 90 polypropylene pots with each pot containing 10 kg of soil and

transplanted with one banana seedling (*Musa AAA Cavendish* cv *Brazil*). Thirty pots were amended with SOF plus plant probiotic, *Tg* (SOF + *Tg*). The population density of strain *Tg* in SOF + *Tg* treatment was confirmed to be  $1.0\text{--}10.0 \times 10^8$  spores g<sup>-1</sup> dry weight of fertilizer at the start of the experiment. Sterilized organic fertilizer (SOF) was amended in half of the remaining 60 pots, and the others received no fertilizer amendment, serving as a control (CK). In SOF and SOF + *Tg* treatments, each pot was supplemented with 200 g organic amendment 1 wk before banana seedlings were transplanted for each of three successive seasons, with each successive season using soil from the previous year after plant removal. The organic fertilizer was produced by chicken manure and rapeseed oil cakes according to the methods described by Wang *et al.* (2013), and the basic properties are as follows: pH 7.8, organic matter 45.5%, water content 28.6%, total N 1.58%, total P 2.82%, and total K 1.21%. Fertilizer sterilization was performed by Co75  $\gamma$ -ray irradiation at Nanjing Xiyue Technology Co. Ltd, Nanjing, China. The sterility of the sterile organic fertilizer was checked by using plate counting method and resulted in no culturable microorganisms after sterilization. Disease incidence was monitored as described by Jeger *et al.* (1995) and calculated as the percentage of infected plants relative to the total number of plants. Plant biomass was determined as described by Shen *et al.* (2019).

### Soil sampling and DNA extraction

Soil-sampling campaigns were performed in the third crop season, and nine soil samples were randomly collected from nine pots, according to method described by Tao *et al.* (2020). One portion of each soil sample was stored at -80°C for DNA extraction, and the other was used for isolation of cultivable fungi. DNA was extracted from 0.5 g soil using PowerSoil DNA Isolation Kit (Qiagen). DNA concentrations were measured using a NanoDrop spectrophotometer (ND-2000; Thermo-Scientific, Wilmington, DE, USA).

### Quantitative PCR analysis

Abundances of total fungi, *Tg*, and *Fusarium oxysporum* were determined using the fungal primers ITS1f/5.8s (Fierer *et al.*, 2005), *Tg* strain-specific primers T-7F/T-7R (Y. Zhang *et al.*, 2019), and *F. oxysporum* group-specific primers FOF1/FOR1 (Jiménez-Fernández *et al.*, 2010), respectively (Supporting Information Table S1). Quantitative PCR amplifications for DNA samples were performed on a 7500 Real-Time PCR System (Applied Biosystems, Pleasanton, CA, USA), according to the manufacturer's instructions (Tables S2, S3). Gene copy numbers were expressed as log<sub>10</sub> values.

### Fungal community tag sequencing, data processing, and OTU table generation

The general universal fungal primers ITS1F (5'-CTTGGTCA TTTAGAGGAAGTAA-3') and ITS2 (5'-GCTGCGTTCTTC ATCGATGC-3') were used to amplify the ITS1 region from soil

DNA (Schoch *et al.*, 2012). The library construction and sequencing on the Illumina MiSeq sequencing platform (Personal Biotechnology Co. Ltd, Shanghai, China) were carried out using previously described protocols (Caporaso *et al.*, 2011; Kozich *et al.*, 2013). Raw sequences were segregated according to the unique barcodes and trimmed of the adaptor and primer sequences in QIIME (Caporaso *et al.*, 2010). After the removal of low-quality reads, forward and reverse sequences were merged. Merged sequences were processed according to the UPARSE pipeline (Edgar, 2013) to generate an operational taxonomic unit (OTU) table (Edgar, 2010). A representative sequence for each OTU was selected (Edgar, 2013) and classified using the RDP classifier against the UNITE Fungal ITS database (Wang *et al.*, 2007).

### Fungal diversity and composition analysis

Chao1 richness indices and Faith's phylogenetic diversity (Faith's PD) (Faith, 1992) were calculated as *Alpha*-diversity metrics in mothur (Schloss *et al.*, 2009). Principal coordinate analysis (PCoA) based on Bray–Curtis dissimilarity matrix was performed to explore patterns of fungal community composition (Oksanen *et al.*, 2012). Differences in community composition across treatments were tested using permutational multivariate analysis of variance (PERMANOVA) (Anderson, 2001). Multiple regression tree (MRT) analysis was conducted to evaluate the effects of organic matter and *Tg* on soil fungal communities (De'ath, 2002).

### Identification of correlations between fungal composition and plant performance

Mantel tests and permutational multivariate analysis of variance (PERMANOVA) analysis were used to identify associations between fungal community composition with plant biomass and disease incidence (Jin *et al.*, 2017). Relationships between biomass and disease incidence with relative abundances of fungal OTUs were identified by Spearman's rank correlation test. To disentangle the potential main biological drivers of plant health and biomass, we identified the main fungal predictors for disease incidence and plant biomass by random forest analysis, according to the method described by Jin *et al.* (2017). Percentage increases in the mean squared error were used to estimate the importance of these responsive fungal OTUs (Jiao *et al.*, 2018).

### Microbial carbon metabolic profiles and fungal microbiome associations

Carbon source utilization capabilities of soil microbial communities were determined using Biolog EcoPlates (Biolog Inc., Hayward, CA, USA), according to method described by Chen *et al.* (2019). Briefly, the assay was conducted by adding 200 µl of soil suspension to each well followed by incubation under aerobic conditions at 25°C. Absorbance readings were taken at 590 nm every 12 h before asymptote was reached. The Biolog EcoPlates consisted of 96-well microplates, containing 31 different carbon

sources plus a blank well including three replications. We subdivided these carbon sources into six group substrates including carbohydrates, carboxylic acids, amino acids, polymers, phenolic acid, and amines/amides for the further analysis. In order to detect relationships between different members of the soil fungal microbiome and their potential combined effects on the capability of soil for utilizing carbon sources, we constructed a network of cooccurring OTUs and deconstructed the fungal community into smaller coherent modules using a weighted gene co-expression network analysis (WGCNA) method to examine module–metabolite relationships (Org *et al.*, 2017).

### Testing effects of different concentrations of *Tg* on soil fungal microbiome via a pot experimental approach

To examine the specific role of *Tg* inoculation in pathogen suppression and changes in the residence fungal communities, we performed a short-term pot experiment in which *Tg* was inoculated into the naturally diseased soil (soil collected from the same field as the microcosm experiment described) at different densities. Four-wk-old banana seedlings were transferred to 1000-ml pots filled with naturally diseased soil pre-inoculated with different concentrations of *Tg*, with final inoculation densities as follows: 0 (Mock),  $1 \times 10^4$  (*Tg1*),  $1 \times 10^5$  (*Tg2*),  $1 \times 10^6$  (*Tg3*),  $1 \times 10^7$  (*Tg4*), or  $1 \times 10^8$  (*Tg5*) spores g<sup>-1</sup> soil. Pots (eight replicates) were placed on small saucers, watered with sterile water, and randomly placed on trays and transferred to a growth chamber (30°C; relative humidity, 80%; photoperiod, 16 h : 8 h, light : dark). Soil fungal microbiome, densities of fungi, *Tg*, and *F. oxysporum* were determined after 2 months of cultivation.

### Fungal community investigated by culture-based methods

Ten gram soil from SOF or SOF + *Tg* was mixed with 100 ml of 0.9% sterile normal saline, shaken for 30 min at 170 rpm in sterile flasks at room temperature, and allowed to stand for 5 min. Tenfold dilutions of the supernatant were prepared, and then, 100 µl of the solution was plated on sterile Petri plates containing Rose Bengal Chloramphenicol (RBC) agar. Plates were incubated at 25°C and checked periodically for fungal growth for up to 10 d. All fungal colonies were transferred to Potato Dextrose Agar (PDA) plates and re-incubated at 28°C. Fungal identification was conducted by morphological and molecular methods according to Singh *et al.* (2018). Taxonomic dendrogram was displayed using iTOL method (Letunic & Bork, 2019).

### Dual culture challenge experiments

A 5 × 5 mm sample of freshly grown *Tg* or *F. oxysporum* f. sp. *Cubense* (FOC) fungal hyphal mat was inoculated on one side of the PDA plate; meanwhile, hyphal mat of fungal isolates recovered from SOF and SOF + *Tg* were inoculated on the opposite side of the plate (Singh *et al.*, 2018). The growth of *Tg*, FOC, and each of fungal isolates cultured alone served as controls. Interactions between *Tg* and FOC with fungal isolates were

scored by measuring colony diameter following 3–10 d postincubation at 25°C.

#### Determination of disease suppression potential of fungal isolates

Four-wk-old banana seedlings were transferred to 1000-ml pots filled with naturally diseased soil (soil collected from the same field as the microcosm experiment described) pre-inoculated with fungal isolates *Humicola* sp. T35 or T37, *Penicillium* sp. 1 or 15, with a final density of  $1 \times 10^6$  spores g<sup>-1</sup> soil. A control treated with water was also established. Pots (nine replicates) were transferred to the growth chamber with identical conditions described above. Disease severity was scored as the density of *F. oxysporum* that colonized plant roots after 2 months of cultivation. *Fusarium oxysporum* densities were determined by suspending 0.1 g rhizosphere soil and plating a dilution series on Komada's medium (Komada, 1975).

#### Effects of *Tg-Humicola* coculture on pathogen invasion resistance

Four-wk-old banana seedlings were transferred to 500-ml pots filled with sterile soil pre-inoculated with *Tg*, *Humicola* sp. T35 or *Penicillium* sp. 1, or a combination of *Tg* mixed with either *Humicola* sp. T35 or *Penicillium* sp. 1. The final inoculation density was  $1 \times 10^6$  spores g<sup>-1</sup> of soil, and for two-strain treatments, the inoculation density was  $0.5 \times 10^6$  spores g<sup>-1</sup> for each strain. A control treated with water was also established. Pots (six replicates) were transferred to the growth chamber with identical conditions described above and watered with sterilized Hoagland solution. After 30 d, banana plants were inoculated with FOC spore suspension ( $1 \times 10^5$  spores g<sup>-1</sup> substrate) or a mock suspension without FOC. Suppression capability was scored by determining the density of FOC colonizing plant roots 4 wk after FOC inoculation (Komada, 1975).

#### Determination of carbon source utilization capability of selected fungal strains and pathogen

Carbon source utilization capabilities of fungi were measured using Biolog FF Microplates system according to Singh (2009). Fungal conidia were produced on PDA plates and collected with sterile cotton-tipped applicators, avoiding carryover of nutrients from the agar medium. Conidia were suspended in the filamentous fungi inoculating fluid broth and adjusted to 75% T (turbidity) by using Biolog turbidimeter. One hundred microliters of each mixture was added to each well of the FF Microplates under aseptic condition. Plates were incubated at 25°C for 7 d before being scored for the presence or absence of carbon source utilization by using Biolog MicroStation. Nutritional similarity between each of the tested fungal strains (*Tg*, *Humicola* sp. T35, and *Penicillium* sp. 1) and fungal consortia (*Tg + Humicola* sp. T35, and *Tg + Penicillium* sp. 1) and FOC was estimated using the following formula for niche overlap index (NOI) (Ji & Wilson, 2002; Wei *et al.*, 2015).

$$NOI = \frac{\text{No. of resources both used by FOC and tested fungal strain or at least one member of the given fungal consortia}}{\text{Total no. of carbon sources utilized by the pathogen FOC}}$$

#### Determination of pathogen suppression by fungal consortia comprised of *Tg* and *Humicola* under different nutrient concentrations

*FOC*, *Tg*, and *Humicola* sp. T35 were grown on PDA plates for 7 d at 28°C to collect fungal spores. Spores were resuspended in sterile normal saline to a final density of  $1 \times 10^7$  spores ml<sup>-1</sup>. Twenty microliters spore suspension of *Tg*, *Humicola* sp. T35, a combination of *Tg* and *Humicola* sp. T35 or 20 µl sterile water, were diluted into 20 ml Potato Dextrose Broth (PDB) (concentrations of 100, 70, 50, 20, or 10%, eight replicates). Each single or coculture was then inoculated with 20 µl FOC spore suspension or sterile water. The single culture and cocultures were incubated at 25°C and 170 rpm on a shaker in a triangular flask. After 7 d, the densities of fungi, FOC, *Tg*, and *Humicola* in each coculture system were determined by qPCR. The pathogen inhibition efficiency was calculated by the percent reduction in pathogen density according to the following formula.

$$Y = \frac{(\text{FOC density in control media} - \text{FOC density in treatment media})}{\text{FOC density in control media}} \times 100$$

We filter sterilized spent media from these cultures with Steriflip Filtration unit (0.22 µm) and determined their pathogen growth inhibition ability using modified dual challenge study. Briefly, 5 × 5 mm pathogen fungal hyphal mat was inoculated on one side of the PDA plate. Meanwhile, 100 µl of sterile spent media was inoculated on the opposite side of the plate by using an Oxford cup. Pathogen growth inhibition ability was assessed by measuring the diameter of the pathogen's colony after 3–10 d postincubation at 25°C. The pathogen cultured alone served as a control.

#### Effects of *Tg-Humicola* coculture on plant-induced systemic resistance

Four-wk-old banana seedlings were transferred to 300-ml pots filled with sterile vermiculite pre-inoculated with *Tg*, *Humicola* sp. T35, or a combination of *Tg* mixed with *Humicola* sp. T35. The final inoculation density was  $1 \times 10^6$  spores g<sup>-1</sup> of vermiculite, and for two-strain treatments, the inoculation density was  $0.5 \times 10^6$  spores g<sup>-1</sup> for each strain. A control treated with water was also established. Pots (nine replicates) were transferred to the growth chamber with identical conditions described above and watered with sterilized Hoagland solution. After 3 d, banana plants were used to determine jasmonic acid (JA) and salicylic acid (SA) contents and the activity of defense enzymes, including chitinase (CHT), peroxidase (POD), phenylalanine ammonia-lyase (PAL), lipoxygenase (LOX), and polyphenol oxidase (PPO). Salicylic acid and JA contents and the activity of defense enzymes were determined according to the methods described by Zhao *et al.* (2020) and Li *et al.* (2021).

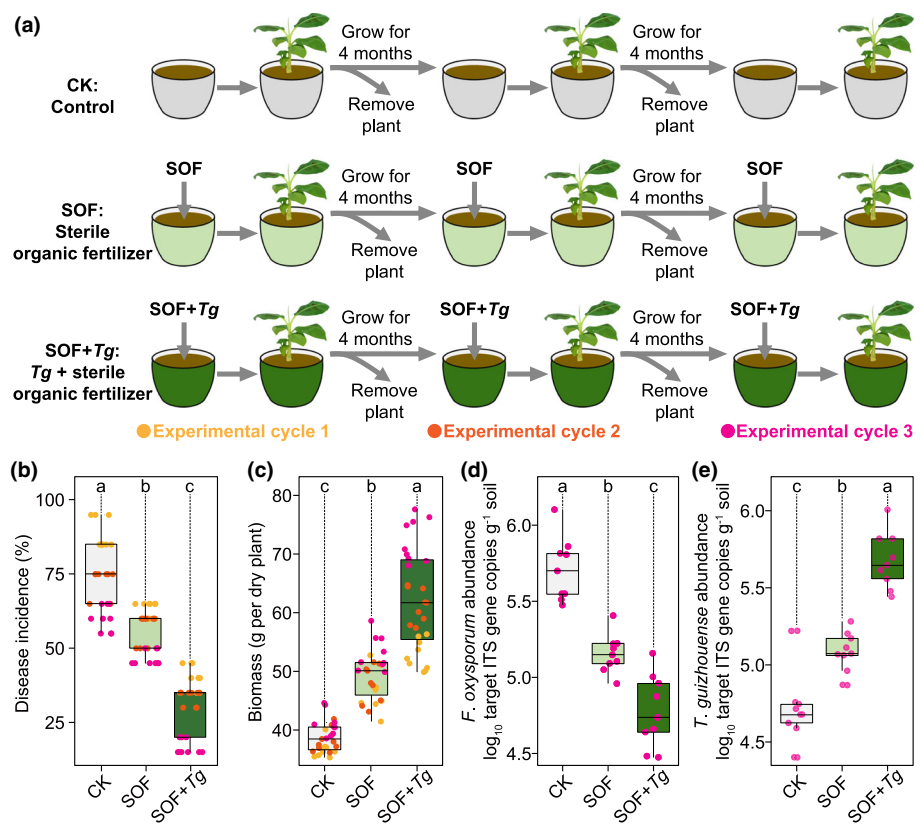


**Fig. 1** Banana plant biomass and Fusarium wilt disease incidence. (a) Experimental scheme of the microcosm experiments for banana cultivation. Average Fusarium wilt disease incidence (b) and banana plant biomass (c) across the three cropping seasons. The abundance of *Fusarium oxysporum* (d) and *Tg* (e) in CK, SOF, and SOF + *Tg* soils in the third crop season. The colors of the dots represent different planting seasons. Different letters indicate a significant difference at the 0.05 probability level according to Tukey's test. CK, control; SOF, sterile organic fertilizer treatment; SOF + *Tg*, *Tg* inoculated sterile organic fertilizer treatment. *Tg*, *Trichoderma guizhouense* NJAU4742. Box plot displays the first and third quartile, with the horizontal bar at the median and whiskers showing the most extreme data point, which is no more than 1.5 times the interquartile range from the box.

## Statistical analyses

Statistical analyses were carried out in R-4.0.3. To determine significant differences, Wilcoxon test or Tukey's HSD test was performed. Linear discriminant analysis (LDA) was performed to identify significant differences in OTUs between fertilization regimes using LefSe (Segata *et al.*, 2011). Taxonomic dendrogram of responsive OTUs (LDA > 2) was displayed using iTOL (Letunic & Bork, 2019). Linear models (LMs) to examine relationships of microbial indicators with disease incidence or biomass and the relative importance for each of the predictors in this model were tested in nutshell and MASS package. Linear regression analyses relating disease incidence or biomass to the selected microbial indicators were performed in basicTrendline package.

## Results

### Banana plant biomass and Fusarium wilt disease incidence

After three successive seasons of banana cultivation (Fig. 1a), the application of organic matter inoculated with or without *Tg* (SOF + *Tg* and SOF) effectively reduced Fusarium wilt disease incidence and increased banana plant biomass as compared to CK (Tukey's test,  $P < 0.05$ , Fig. 1b,c). The disease control and plant growth promotion of SOF + *Tg* were higher than SOF treatment, with average values of 59.09% and 60.47%, respectively. For each cropping season, SOF + *Tg* treatment showed the highest biomass and lowest disease incidence compared with

other treatments (Tukey's test,  $P < 0.05$ , Fig. S1a,b). In the third season, disease control and growth promotion in SOF + *Tg* treatment were  $72.2 \pm 3.9\%$  and  $76.4 \pm 8.5\%$ , respectively.

### Fungal community abundance

For soils sampled in the third season, total fungal abundance was significantly higher in the SOF + *Tg* treatment vs the CK (Fig. S2). The abundance of *F. oxysporum* was significantly lower in the SOF + *Tg* treatment, as compared to SOF and CK, respectively (Tukey's test,  $P < 0.05$ , Fig. 1d). We used real-time qPCR, fungal ITS amplicon sequencing and culture-based experiments to examine whether *Tg* had successfully colonized the soil in our experiments. Results showed that SOF + *Tg* treatment had the highest levels of *Tg* (Tukey's test,  $P < 0.05$ ), with an average gene copy value of  $5.68 \text{ g}^{-1}$  soil after logarithmic transformation, whereas these values were 5.09 and 4.71, respectively, for the SOF and CK (Fig. 1e). Fungal ITS amplicon sequencing results showed that *Trichoderma* OTU5 was significantly enriched in SOF + *Tg* treatment, displaying 99.30% sequence identity with *Tg* (Fig. S3a). In cultural-dependent experiments, four fungal isolates from SOF + *Tg* soil displayed 100% sequence identity with *Tg* and could be identified as being this strain (Fig. S3b). Furthermore, disease incidence was significantly and positively correlated with *F. oxysporum* abundance and negatively correlated with *Tg* abundance. Plant biomass was significantly and positively correlated with total fungi and *Tg* abundance, while negatively correlated with *F. oxysporum* abundance (Fig. S4).

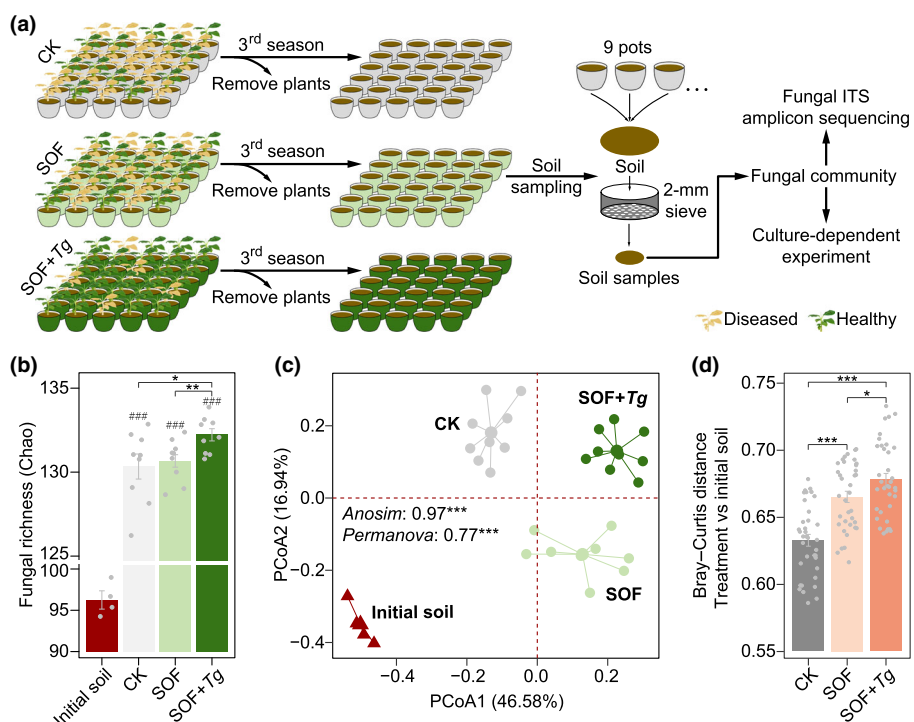


**Fig. 2** Fungal community diversity and structure. (a) Experimental scheme for sampling of soils for Fungal ITS amplicon sequencing and culture-based experiments in the third crop season. (b) Fungal richness (Chao1) among all soil samples (mean  $\pm$  SE). (c) Principal coordinate analysis (PCoA) ordinations of fungal community composition based on Bray–Curtis distance metric among all soil samples. (d) Fungal community dissimilarities between treatments and initial soil samples (mean  $\pm$  SE). VS, represents vs number sign indicates significant differences between a given treatment (CK, SOF, and SOF + Tg) and initial soil (Wilcoxon test: #,  $P < 0.001$ ); while asterisks indicate significant differences between CK, SOF, and SOF + Tg (Wilcoxon test): \*,  $P < 0.05$ ; \*\*,  $P < 0.01$ ; \*\*\*,  $P < 0.001$ . Differences in fungal Beta diversity of initial soil, CK, SOF, and SOF + Tg treated soils were determined by analysis of permutational multivariate analysis of variance (PERMANOVA) and analysis of similarities (ANOSIM). CK, control; SOF, sterile organic fertilizer treatment; SOF + Tg, Tg inoculated sterile organic fertilizer treatment; Tg, *Trichoderma guizhouense* NJAU4742.

### Fungal community diversity and structure

Soil sampled from the third crop season was used to examine whether *Tg* and organic matter inputs indirectly change the composition, diversity, and functioning of indigenous fungal microbiome (Fig. 2a). Significant higher fungal richness (Chao1) and diversity (Faith's PD) indices were observed in CK, SOF, and SOF + *Tg* soils as compared to initial soil (Wilcoxon test,  $P < 0.05$ , Figs 2b, S5a). Chao1 and Faith's PD indices did not differ significantly between CK and SOF, while SOF + *Tg* treatment significantly increase the Chao1 index as compared to CK and SOF treatments and increase Faith's PD index as compared to SOF treatment (Wilcoxon test,  $P < 0.05$ , Figs 2b, S5a).

Principal coordinate analysis results clearly showed significant differences in the fungal community composition among initial soil, CK, SOF, and SOF + *Tg* treatments (PERMANOVA and ANOSIM tests,  $P < 0.001$ , Fig. 2c). Overall, fungal community composition from initial soils was distinctly separated from CK, SOF, and SOF + *Tg* soils along the first component (PCoA1) and from CK and SOF + *Tg* along the second component (PCoA2). Fungal community composition from SOF + *Tg* was distinctly separated from CK along PCoA1 and from SOF along PCoA2. Bray–Curtis distances between SOF + *Tg* and initial soils were significantly higher than those observed in the comparison of SOF and CK vs initial soils, respectively, while the lowest

Bray–Curtis distances between CK and initial soils were observed (Wilcoxon test,  $P < 0.05$ , Fig. 2d).

Multiple regression tree analysis showed fungal communities could be split into two major groups according to whether or not they had been inoculated with *Tg*, with a further separation of SOF and CK. The factor SOF + *Tg* input produced the largest deterministic effects, explaining 37.58% of the overall variation in fungal community composition (Fig. S5b). PERMANOVA and ANOSIM tests also confirmed the significant effects of SOF + *Tg* ( $P < 0.001$ , Table S4).

### Fungal community composition variation

Significant differences in fungal community compositions were observed in initial, CK, SOF, and SOF + *Tg* soils. Higher relative abundance of Ascomycota and Chytridiomycota was observed in the initial soil as compared to CK, SOF, and SOF + *Tg* soils. CK and SOF significantly increased the relative abundance of Basidiomycota and Glomeromycota, respectively, as compared to initial soil and other treatments. SOF + *Tg* treatment significantly decreased the relative abundance of *Fusarium* as compared to initial, CK, and SOF soils, while the highest relative abundance of *Fusarium* was observed in the initial soil (Fig. 3a).

After discarding low-abundance OTUs with a relative abundance  $< 0.01\%$  in all soil samples and nonfungal OTUs, a total

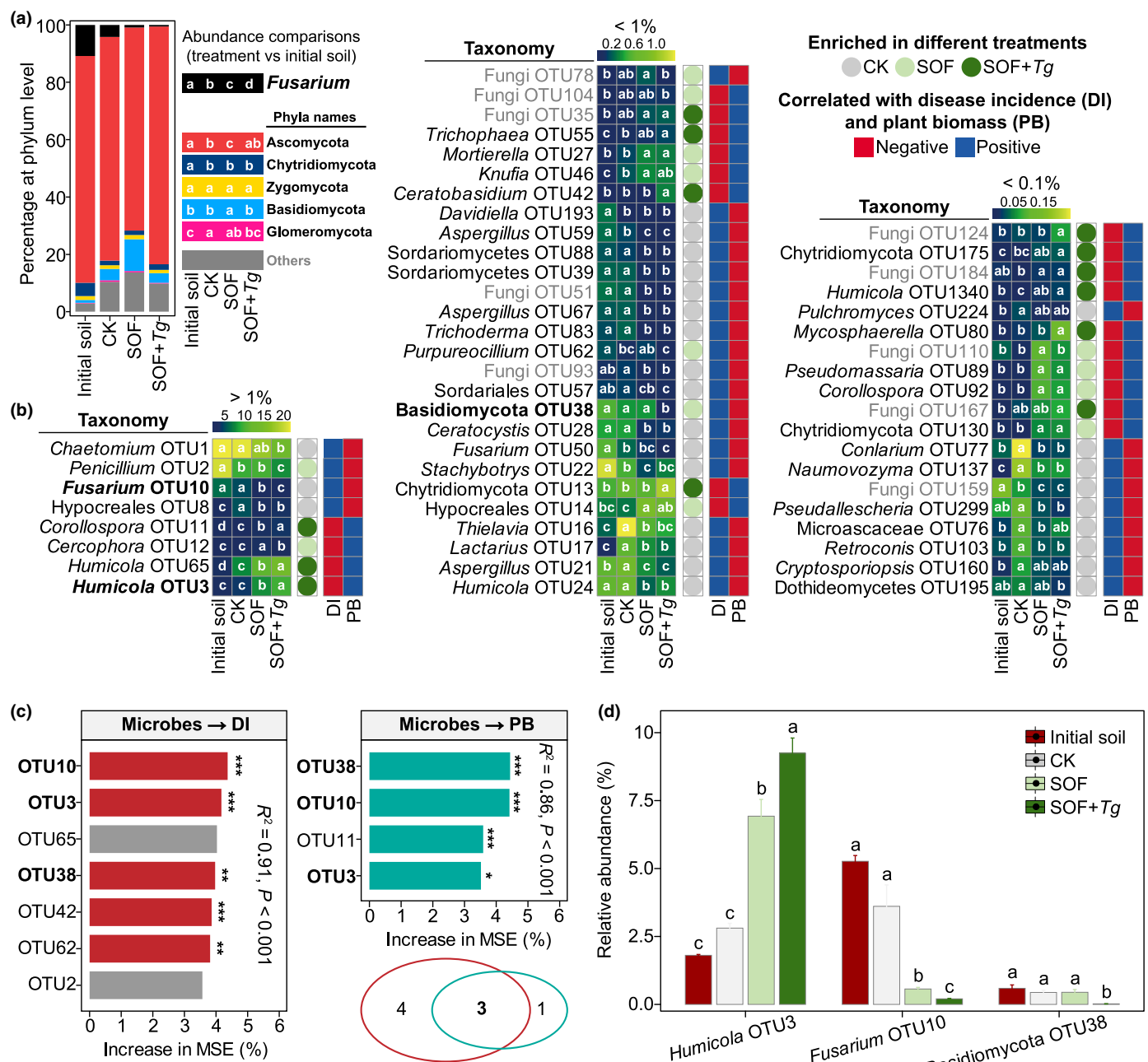


**Fig. 3** Fungal community composition variation and potential fungal predictors of plant disease and growth. (a) The relative abundance of the pathogen (black) and other fungal phyla (other colors) in initial, CK, SOF, and SOF + Tg soils. (b) Heatmaps showing the core fungal microbiome influenced by fertilization regimes and significantly correlated with plant biomass and disease incidence. Color circles represent operational taxonomic units (OTUs) responding significantly to CK, SOF, and SOF + Tg treatments, respectively (linear discriminant analysis (LDA)  $> 2$ ,  $P < 0.05$ ), and color squares show OTUs that were significantly correlated with disease incidence and plant biomass. (c) Random forest mean predictor importance (percentage of increase in mean square error) of the model selection of fungal OTUs as drivers for the Fusarium wilt disease incidence (DI) and banana plant biomass (PB). Percentage increases in the mean squared error (MSE) of variables were used to estimate the importance of these predictors, and higher MSE% values imply more important predictors. Significance levels are as follows: \*,  $P < 0.05$ ; \*\*,  $P < 0.01$ ; \*\*\*,  $P < 0.001$ . Venn diagrams showing the unique and shared fungal OTUs in the two models. (d) The relative abundance of the three shared fungal OTUs in initial, CK, SOF, and SOF + Tg soils (mean  $\pm$  SE). Different letters indicate a significant difference at the 0.05 probability level according to Tukey's test ( $n = 9$ ). CK, control; SOF, sterile organic fertilizer treatment; SOF + Tg, *Trichoderma guizhouense* NJAU4742.

of 1728 fungal OTUs were recovered, with 134 OTUs being identified as core OTUs based on their presence in at least 80% of all samples. Based on LDA, we found the relative abundance of 96 core fungal OTUs was significantly influenced by the

application of SOF and Tg, in which 24 core fungal OTUs were enriched in SOF + Tg treatment as compared to SOF and CK (Fig. S6). Spearman's correlation analysis found that the relative abundances of 54 core fungal OTUs were significantly correlated

with disease incidence and plant biomass, in which 22 OTUs showed negative and positive relationships with disease incidence and plant biomass, respectively, and were thus deemed to be potentially beneficial fungi. In particular, 13 potentially beneficial fungal OTUs were significantly enriched in SOF + *Tg* treatment (Fig. 3b). The relative abundances of these 13 fungi in initial soils were significantly lower than that in SOF + *Tg* soils (Tukey's test,  $P < 0.05$ , Fig. 3b).

### Linking fungal community and microbial carbon metabolism

Significant differences in microbial carbon metabolism capability were observed in soils from CK, SOF, and SOF + *Tg* (Fig. S7a,b). SOF + *Tg* treatment significantly increased the soil microbial carbon metabolism by up to 23.98 and 38.91% as compared to CK and SOF, respectively. The utilization rates of six groups of substrates including carbohydrates, carboxylic acids, amino acids, polymers, phenolic acid, and amines/amides were significantly negatively correlated with disease incidence, while the utilization rates for these carbon sources were positively correlated with plant biomass (Fig. S7c,d).

Weighted gene co-expression network analysis found that the variation of fungal community composition was significantly correlated with the capability of soil microbes for utilizing carbon sources (Fig. S8). Although there were more modules in SOF networks, the numbers of nodes and edges were significantly increased in SOF + *Tg* networks (Fig. S8a–d). The module-metabolite association analysis indicated a strong correlation between fungal community composition and resource utilization (Fig. S8e). In SOF + *Tg* networks, fungal module I was significantly positively correlated with carbohydrates, carboxylic acids, amino acids, polymers, phenolic acid, and amine utilization. Furthermore, significant negative and positive relationships between fungal module I with disease incidence and plant biomass were observed, respectively. In SOF networks, both fungal modules I and II showed positive correlations with amines, phenols acid, polymers, and carboxylic acids utilization. However, significant positive and negative relationships between these fungal modules with disease incidence and plant biomass were observed, respectively (Fig. S8e).

### Potential fungal predictors of plant disease and growth

Both the results of mantel and permutational multivariate analysis of variance (PERMANOVA) tests showed that soil fungal community composition was significantly correlated to plant biomass and disease incidence (Table S5). Similarly, of the indicators explored by LM analysis for their contribution to disease incidence and plant biomass, fungal richness (Chao1), and community structure (PCoA1) were observed to be most important in the two respective models (Table S6). We also found that Chao1 and PCoA1 showed significant negative relationships with disease incidence, while significantly and positively impacted plant biomass (Fig. S9a,b).

The random forest models resulted in the selection of seven and four fungal OTUs as the main microbial predictors of disease

incidence and plant biomass, respectively (Fig. S10a,b). OTU10, which was identified as *Fusarium*, was found to be the most important variable for predicting disease incidence followed by *Humicola* OTU3, Chaetomiaceae OTU65, Basidiomycota OTU38, *Ceratobasidium* OTU42, *Purpureocillium* OTU62, and *Penicillium* OTU2 (Fig. 3c). With regard to plant biomass, Basidiomycota OTU38, *Fusarium* OTU10, *Corollospora* OTU11, and *Humicola* OTU3 were identified as potential biological predictors (Fig. 3c). Furthermore, these observations were supported by LM analysis, which showed that OTU3, OTU10, and OTU38 were potentially important predictors to disease incidence and plant biomass (Table S6).

In particular, OTU3, OTU10, and OTU38 were shared in the two random forest models, and we therefore selected these taxa for follow-up analyses. Significantly, higher relative abundance of OTU3 was observed in SOF + *Tg*, while lower relative abundances of OTU10 and OTU38 were observed, as compared to initial, CK, and SOF soils (Tukey's test,  $P < 0.05$ , Fig. 3d). The relative abundance of OTU10 and OTU38 was significantly and positively correlated with disease incidence, while OTU3 was negatively correlated with disease incidence (Fig. S11). Moreover, all responsive OTUs were also significantly correlated with plant biomass.

### *Tg* specificity and effects on soil fungal community and pathogen suppression

Increasing inoculation amount of *Tg* significantly increased the population density of this fungus, as well as the percentage of *Tg* in fungal community (Tukey's test,  $P < 0.05$ , Figs 4a, S12a). However, increasing inoculation density of *Tg* above  $10^4$  g<sup>-1</sup> dry soil did not result in a significant increased level of pathogen suppression, with the highest inoculation levels showing only modestly reduced densities of pathogen as compared to mock inoculation (Figs 4b, S12b).

The presence of *Tg* had a large effect on fungal community composition determined at the end of the pot experiment (PERMANOVA and ANOSIM tests,  $P < 0.001$ , Fig. 4c). Specifically, the application of *Tg* significantly affected the composition of *Humicola* group by enriching the relative abundance of potentially beneficial fungal taxa OTU3 and OTU 2648, while decreasing the relative abundance of OTU932 and OTU53 (Tukey's test,  $P < 0.05$ , Fig. 4d). Furthermore, the relative abundance of *Humicola* OTU3, OTU2648, and OTU1872 showed similar trends in response to the application of different amounts of *Tg* (Fig. 4e), which confirmed that some specific *Humicola* species could be stimulated by the appropriate level of *Tg* inoculation. Fungal diversity and overall taxonomic composition were also significantly influenced by the different levels of *Tg* inoculation (Fig. S12c–i).

### Fungal isolates recovered from SOF and SOF + *Tg* soils

A total of 41 species could be detected among the 114 strains isolated from SOF + *Tg* soil, with 97% of isolates belonging to Ascomycota and 3% to Basidiomycota. From the 71 SOF-

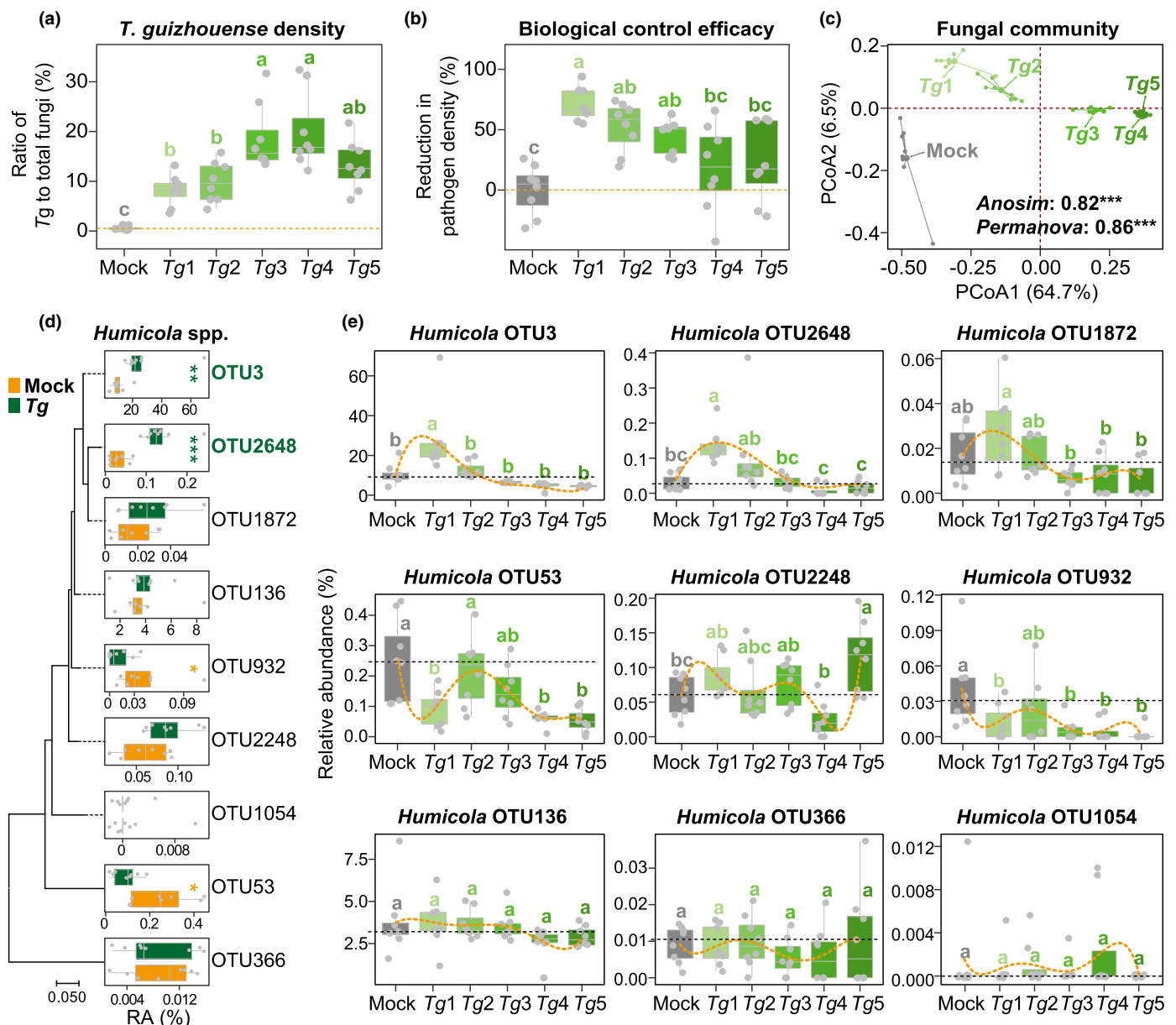


**Fig. 4** *Tg* specificity and effects on soil fungal community and pathogen suppression. Population densities of *Tg* (a) and *Fusarium oxysporum* (b) in soils amended with different concentrations of *Tg*. (c) Principal coordinate analysis (PCoA) ordinations of fungal community composition based on Bray–Curtis distance metric across all soil samples. (d) Taxonomic dendrogram of all *Humicola* operational taxonomic units (OTUs) detected by fungal ITS amplicon sequencing. Boxplot showing the relative abundance of *Humicola* OTUs in the soil inoculated with *Tg* ( $10^4$  spores  $g^{-1}$  dry soil) or sterile water (Wilcoxon test: \*,  $P < 0.05$ ; \*\*,  $P < 0.01$ ; \*\*\*,  $P < 0.001$ ). (e) Relative abundance of *Humicola* OTUs in soils amended with different concentrations of *Tg*. The biological control efficacy was quantified as percent reduction in pathogen density in soil. Different letters indicate significant differences at the 0.05 probability level according to Tukey's test ( $P < 0.05$ ). Mock, sterile water; *Tg*1, *Tg*2, *Tg*3, *Tg*4, *Tg*5, soil inoculated with *Tg* at concentrations of  $10^4$ ,  $10^5$ ,  $10^6$ ,  $10^7$ , and  $10^8$  spores  $g^{-1}$  dry soil, respectively. *Tg*, *Trichoderma guizhouense* NJAU4742. Box plot displays the first and third quartile, with the horizontal bar at the median and whiskers showing the most extreme data point, which is no more than 1.5 times the interquartile range from the box. The curve shows the variation trend of *Humicola* relative abundance.

derived isolates, 26 fungal species could be distinguished, with 89% belonging to Ascomycota and 11% to Basidiomycota (Fig. S13a,b). *Trichoderma* dominated the fungal species recovered from SOF + *Tg* soil, followed by *Aspergillus*, *Humicola*, *Alternaria*, and other fungal genera. *Penicillium* dominated the fungal species recovered from SOF soil, followed by *Fusarium*, *Aspergillus*, *Filobasidium*, and other fungal genera (Fig. S13c).

Particularly, six of the 11 most dominant fungal genera based upon sequencing data (relative abundance  $> 1\%$ ) were recovered as isolates from these samples. Moreover, the relative rate of recovery of isolates from five of these dominant fungal genera (*Penicillium*, *Trichoderma*, *Fusarium*, *Humicola*, and *Chaetomium*) followed sequence-based trends of relative abundance across SOF and SOF + *Tg* treatments (Fig. S13c).

## Tg and pathogen inhibition assays

The isolates recovered from SOF and SOF + *Tg* treatments were assayed for their ability to inhibit the growth of pathogen, FOC, and the probiotic strain, *Tg* (Fig. S14). In total, > 80% of the FOC-suppressing fungal strains were derived from the genera *Trichoderma*, *Penicillium*, *Aspergillus*, and *Humicola*, whereas *Tg*-suppressing fungal isolates were only from two genera, namely *Aspergillus* and *Penicillium* (Table S7). The proportion of isolates recovered from SOF + *Tg* soil that could inhibit FOC was significantly higher than observed for isolates cultivated from SOF soil (Wilcoxon test,  $P < 0.05$ , Fig. 5a). There was no significant difference between SOF and SOF + *Tg* treatments in terms of proportion of isolates that inhibited *Tg*, with only 8.45 and 5.18% of fungal isolates showing inhibition, respectively (Fig. 5b).

## Pathogen suppression potential of selected fungal isolates

We selected four fungal isolates from our collection that showed FOC inhibition to examine their ability to inhibit banana root infection of pathogen in pot cultures. These included two isolates that corresponded to OTU3, which was a highly responsive OTU affiliated with genus *Humicola*, and two *Penicillium* isolates, as this genus was the most dominant in our collection. We grew sterile banana plants in naturally diseased soil that was pre-inoculated with one of the targets *Humicola* or *Penicillium* strain and tracked pathogen population density on plant roots. The two *Humicola* strains, T35 and T37, significantly reduced the density of *Fusarium* on banana roots in comparison with the noninoculated control, while the two *Penicillium* strains, 1 and 15, did not have any significant effect on *Fusarium* density (Fig. 5c).

## Effects of co-inoculation of *Tg* plus selected fungal isolates

We further investigated the pathogen suppression capabilities of co-inoculations of selected fungal strains (*Humicola* sp. T35 and *Penicillium* sp. 1) together with *Tg*. As observed in the previous assays, *Tg* and *Humicola* sp. T35 each reduced FOC density on banana roots when inoculated separately, while this was not the case for *Penicillium* sp. 1 (Fig. 5d). The combination of *Tg* plus *Humicola* sp. T35 showed the strongest suppression to FOC, while the co-inoculation of *Tg* plus *Penicillium* sp. 1 showed only a modest level of FOC suppression.

We then examined the extent to which fungal resource competition patterns could explain the observed levels of pathogen suppression by individual strains and co-inoculations. Results showed that pathogen suppression levels were significantly and positively correlated with the NOI of the inoculum (Fig. 5e,f). We furtherly noticed that the pathogen suppression ability of *Tg* and *Humicola* sp. T35 is related to their potential ability to compete for carbohydrate, carboxylic acid, miscellaneous, and polymer with pathogen FOC. Niche overlap indexes between FOC and the given fungi in the four groups of substrates are significantly negatively correlated with the density of FOC (Fig. 5g).

## Impacts of nutrient availability on pathogen suppression of fungal consortia

As observed in our assays, the co-inoculation of *Tg* and *Humicola* sp. T35 could significantly reduce FOC density on banana roots, and niche overlap with the pathogen was highlighted as a potential driving mechanism. Given the suggested involvement of resource competition, we further investigated the impact of resource availability on the pathogen suppression capabilities of co-inoculation of *Tg* and *Humicola* sp. T35 (Fig. 6a). In full-strength normal PDB medium, co-inoculation of *Humicola* sp. T35 and *Tg* showed the strongest suppression to FOC (Fig. 6b), while the fungal inhibition ability of filter sterilized spent culture media (produced in the presence and absence of pathogen) did not show the same trends (Figs 6c, S15a), suggesting that enhancement of pathogen growth inhibition was not driven by fungal antagonistic activity. In particular, when grown in coculture systems, both the population density of *Tg* or *Humicola* sp. T35 showed no significant difference as compared to when cultured alone (Fig. 6d), showing that these fungi did not affect each other's growth.

Interestingly, when grown at lower nutrient concentrations (50 and 70% PDB), co-inoculation of *Humicola* sp. T35 and *Tg* enhanced the efficiency of pathogen inhibition as compared to full-strength medium (Figs 6e, S15b). The ratio of resident fungi to FOC population density strongly explained the observed levels of pathogen suppression enhancement, but not the pathogen growth inhibition activity of the fungal spent media (Figs 6e, S15c), suggesting the pathogen growth inhibition by resident fungi was predominantly driven by niche competition. We subsequently used an exploitation competition model to show that *Tg* and *Humicola* could synergistically act toward reducing resource availability for FOC, thereby negatively affecting FOC density (Fig. 6f).

## Induction of plant systemic resistance by fungal consortia

We noticed that the inoculation of *Tg*, *Humicola* sp. T35, and the combination of *Tg* and *Humicola* sp. T35 could significantly increase JA and SA contents in banana plants as compared to control. In particular, the combination of *Tg* plus *Humicola* sp. T35 showed the highest levels of JA and SA, while the inoculation of *Tg* and *Humicola* sp. T35 did not differ significantly (Fig. 7a). We also examined the activities of CHT, POD, PAL, LOX, and PPO after inoculating the plants with fungal consortia or single species. All treatments increased the average values of CHT, POD, PAL, LOX, and PPO activities as compared to control. The activities of CHT, POD, PAL, LOX, and PPO in banana plants inoculated with the combination of *Tg* and *Humicola* sp. T35 were higher than those of banana plants inoculated with single species of *Tg* and *Humicola* sp. T35 (Fig. 7a). These data indicate that the defense system in banana plants is more responsive to the inoculation of the combination of *Tg* and *Humicola* sp. T35.

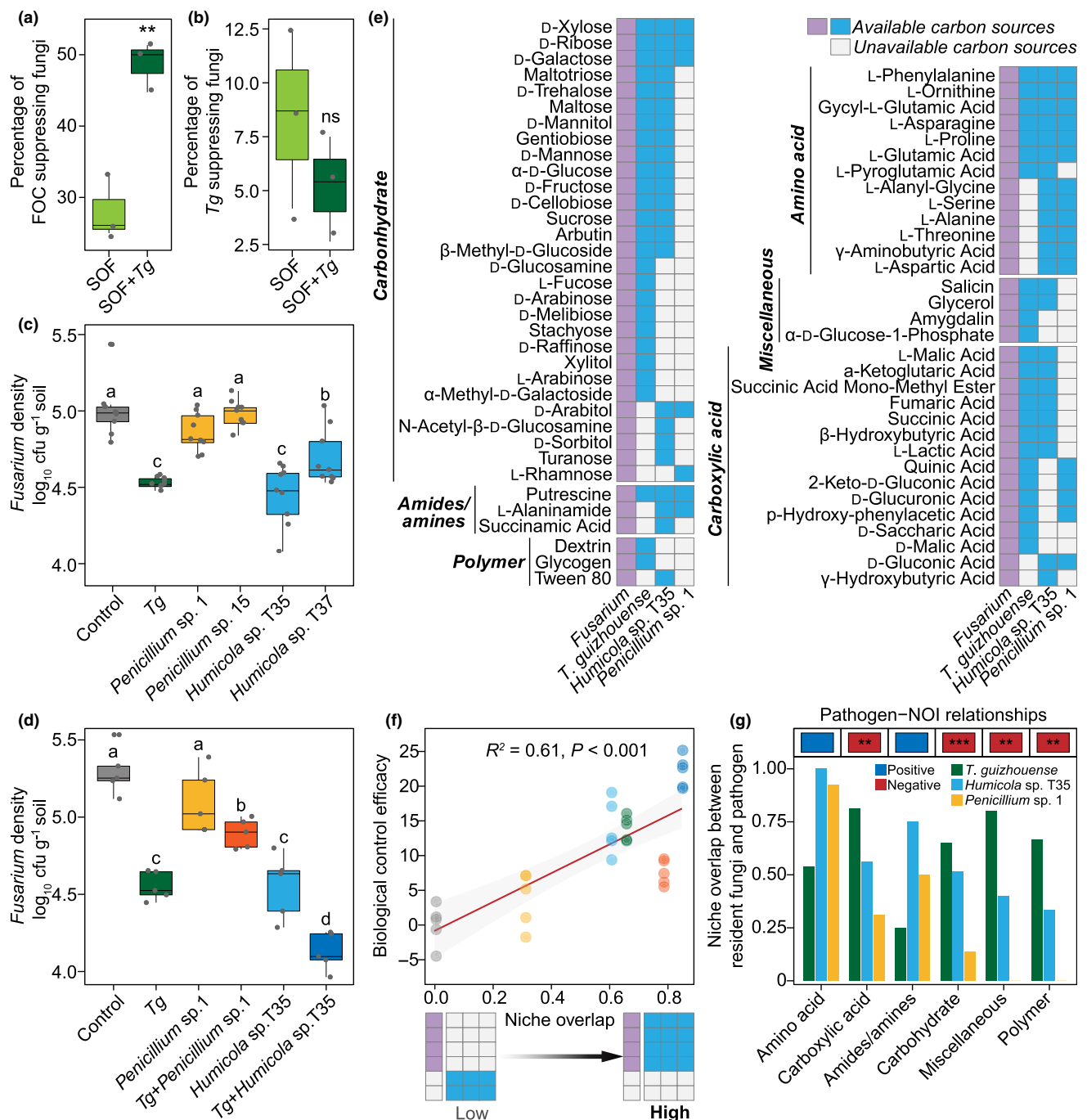


**Fig. 5** Effects of co-inoculation of *Tg* plus selected fungal isolates on pathogen suppression. Percentage of isolates from the sterilized organic fertilizer (SOF) and SOF + *Tg* treatments that can inhibit the growth of FOC (a) and *Tg* (b) ( $n = 3$ , Wilcoxon test: \*\*,  $P < 0.01$ ; ns, not significant). SOF, sterile organic fertilizer treatment; SOF + *Tg*, *Tg* inoculated sterile organic fertilizer treatment. (c) Population densities of *Fusarium* in the naturally diseased soil amended with either *Tg*, *Penicillium* strain 1 or 15, or *Humicola* strain T35 or T37. (d) FOC density on plant roots growing in sterile soil pre-inoculated with the given strains (*Tg*, *Penicillium* sp. 1, and *Humicola* sp. T35) and their combination (*Tg* + *Penicillium* sp. 1, and *Tg* + *Humicola* sp. T35). Different letters indicate significant differences at the 0.05 probability level according to Tukey's test ( $P < 0.05$ ). (e) A schematic matrix capturing resource competition interactions between the pathogen (purple boxes) and given fungal species (blue boxes). Colored squares indicate that the given fungi consume a given resource. (f) Relationship between biological control efficacy and niche overlap index (NOI). Symbol colors correspond to the treatment designations given in (d). The biological control efficacy was quantified as percent reduction in pathogen FOC density on roots. (g) Niche overlap index between the pathogen and given fungal species in the six groups of substrates including carbohydrate, carboxylic acid, amino acid, amides/amines, miscellaneous, and polymer; color block with asterisks indicated the relationships between pathogen density and NOI. Niche overlap index was the similarity in resource utilization between FOC with these selected fungal strains and fungal consortia. FOC, *Fusarium oxysporum* f. sp. *Cubense*; *Tg*, *Trichoderma guizhouense* NJAU4742. Box plot display the first and third quartile, with the horizontal bar at the median and whiskers showing the most extreme data point, which is no more than 1.5 times the interquartile range from the box.

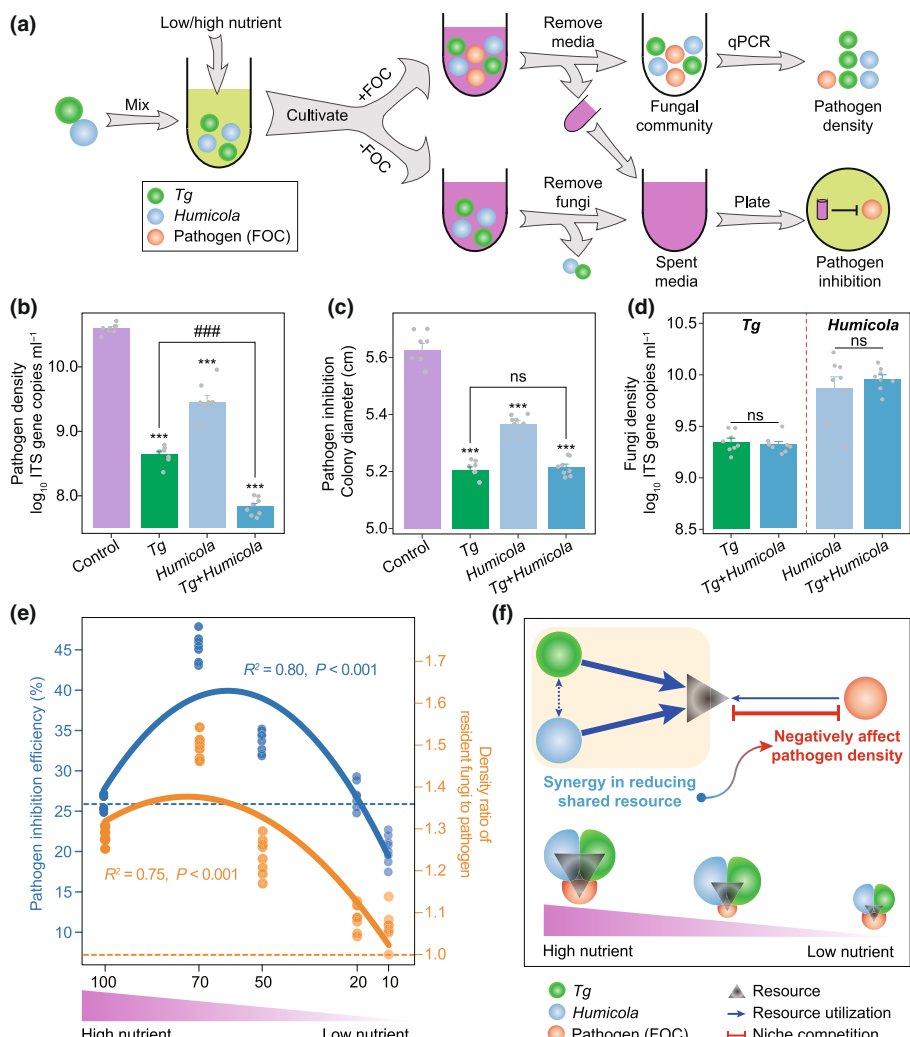


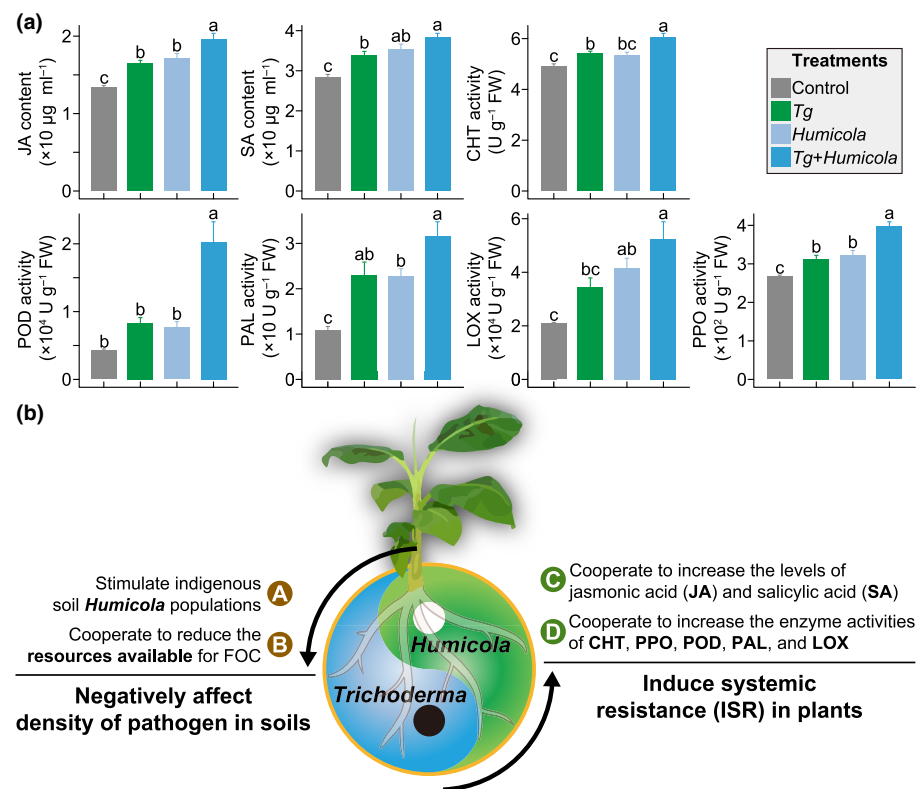
**Fig. 6** Impacts of nutrient availability on pathogen suppression of fungal consortia. (a) Schematic representation of the experimental design. (b) The pathogen density in cocultures (mean  $\pm$  SE). (c) The colony diameter of the pathogen in dual challenge assays (mean  $\pm$  SE). (d) Population densities of *Tg* and *Humicola* in cocultures (mean  $\pm$  SE). Asterisks indicate significant differences between a given treatment and the control as determined by the Wilcoxon test: \*\*\*,  $P < 0.001$ ; while number sign indicates significant differences between *Tg* and *Tg* + *Humicola* as determined by the Wilcoxon test: ###,  $P < 0.001$ ; ns, not significant. (e) Pathogen inhibition efficiency of fungal consortia (comprised of *Tg* and *Humicola*) and the density ratio of resident fungi to pathogen in the media with different nutrient concentrations. Pathogen inhibition efficiency was quantified as percent reduction in pathogen FOC density. (f) Exploitation competition model depicting cooperative impacts of *Tg* and *Humicola* on pathogen density reduction via resource competition. FOC, *Fusarium oxysporum* f. sp. *Cubense*; *Tg*, *Trichoderma guizhouense* NJAU4742.

## Discussion

In this study, we examined the impacts of fungal probiotics amended biofertilizer on disease suppression within a continuous banana monoculture cropping system in a naturally diseased soil. To eliminate the impacts of native fertilizer microbiome, we imposed treatments with *T. guizhouense* NJAU4742 (*Tg*) in the presence and absence of SOF. Our objective was to disentangle the progressive impact of *Tg* on the development of disease suppression and identify the manipulatable components and functioning of the soil fungal microbiome that contribute to disease suppression. Our study showed that *Tg*-amended biofertilizer (SOF + *Tg*) significantly enhanced the banana plant growth and health. We further found that *Tg* could reduce the pathogen density within naturally diseased soil in the presence and absence of organic fertilizer inputs. We demonstrated that the disease suppression action of *Tg*-amended biofertilizer was the sum of direct pathogen suppression by *Tg* and the indirect effects due to interactions with resident fungi (e.g. *Humicola*) in resource competition with pathogen and in induction of plant systemic resistance (Fig. 7b).

Microorganisms are important indicators of soil health (Yuan *et al.*, 2020), and changes in microbial diversity, as well as distinct shifts in the microbial composition, have been linked to disease suppression (Kwak *et al.*, 2018; Lee *et al.*, 2021). We also found links between changes in fungal diversity and community composition with banana plant performance. SOF + *Tg* treatment significantly increases fungal richness and Faith's PD, which was associated with lower disease incidence. Similar patterns have been found in comparisons of disease-suppressive vs disease-conducive soils (Mendes *et al.*, 2011), and higher fungal diversity was found in roots of healthy winter wheat plants as compared to diseased plants (Lemanczyk & Sadowski, 2002). Several previous studies have also reported that higher bacterial diversity in biofertilization patterns related to the suppression of soilborne diseases (Fu *et al.*, 2017; Xiong *et al.*, 2017; Li *et al.*, 2020), and our observation of lower pathogen densities and disease incidence in SOF + *Tg* support these findings.

Previous studies have demonstrated that differences in microbial community composition can be linked to the disease-suppressive capacity of soils (Raaijmakers & Mazzola, 2016), as well as the ability to promote plant growth (Jin *et al.*, 2017).



Similarly, our PCoA and multiple regression tree analyses showed clear shifts in fungal community composition as related to fertilization, banana wilt disease severity, and plant biomass. We found 22 fertilization-stimulated fungal OTUs were significantly negatively correlated with disease incidence; of those, 13 fungal OTUs were significantly enriched in SOF + *Tg* soils. Notably, these results were further conformed by our culture-based experiments, which found that a greater proportion of pathogen-suppressing fungal isolates were recovered from SOF + *Tg* soils as compared to SOF soils. These findings are in accordance with previous studies, which reported that *Trichoderma*-amended biofertilizers application could suppress soilborne diseases by regulating the indigenous microbial community compositions (Qiu *et al.*, 2012; Xiong *et al.*, 2017; Li *et al.*, 2020). Observed shifts in community composition were also reflected in carbon resource utilization patterns, with SOF + *Tg* showing the highest carbon resource utilization. Such increased resource utilization ability may enhance plant health via improvements in nutritional status and/or greater suppression of pathogens invasion via resource competition (Wei *et al.*, 2015; Yang *et al.*, 2017). These results demonstrated that rehabilitation or augmentation of beneficial host-associated fungal microbiome induced by biofertilizer may be an effective means to control plant diseases.

Although changes in soil functioning with respect to disease suppression may involve broad and complex shifts in microbial community, it has also been observed that soil suppressiveness may stem from changes in population densities of specific microbial taxa (Kwak *et al.*, 2018; Lee *et al.*, 2021). Our results suggested that *Tg*-amended biofertilizer could specifically stimulate indigenous beneficial fungi that contribute to plant health. In

particular, OTU3, belonging to *Humicola*, was the most important variable for predicting disease suppression and plant growth promotion and also represented a key taxon within microbe-metabolite interactions network. Notably, we further demonstrated that the density of *Humicola* spp. could be stimulated by introduction of *Tg* both in the presence and absence of organic matter inputs. This result is in line with previous reports that some PGPR can stimulate indigenous beneficial bacteria as cooperative partners and assist in plant health (Hu *et al.*, 2021; Sun *et al.*, 2021), and our work extends this action to fungi.

For a more direct examination of the role of resident soil fungal populations in the suppression of FOC, we recovered and characterized fungal isolates from SOF and SOF + *Tg* soils. A number of our isolates corresponded to the OTUs that were detected by high-throughput tag sequencing, including inoculated strain *Tg* and some highly responsive fungi such as *Humicola* OTU3. We therefore tested the ability of these isolates to inhibit FOC in plate and pot assays. Indeed, selected *Humicola* isolates were able to suppress FOC *in vitro* and in natural soil. It has been reported that some *Humicola* species have the capability of secreting hydrolysis enzymes to promote the degradation of lignocellulose (Kogo *et al.*, 2017). Here, this genus is implicated for the first time in plant disease suppression.

Cooperative interactions between *Trichoderma* and other biological agents, for instance *Pseudomonas*, *Bacillus*, and *Glomus*, were previously reported to enhance the biocontrol efficiency (Jambhulkar *et al.*, 2018; Matrood *et al.*, 2020; Zhou *et al.*, 2021). Similarly, we noticed that the combined inoculation of *Humicola* together with *Tg* yielded the highest level of pathogen suppression. Thus, it appears that the effectiveness of *Tg*

amended biofertilizer stems not only from the action of *Tg*, but also from the stimulation of resident fungal populations that together with *Tg* serve to provide a higher level of disease protection. These results are in line with several recent reports that have shown plant protection can be the product of the combined actions of microbial taxa (Hu *et al.*, 2016; Saleem *et al.*, 2019).

Notably, we found that high niche overlap between the pathogen and stimulated resident fungi, as determined by resource utilization patterns, had a high degree of explanatory power with respect to the level of pathogen suppression. We therefore developed an exploitation competition model to illustrate this potential niche overall mechanism of pathogen suppression. This model highlights the role of plant-beneficial fungal consortia, comprised of the introduced fungal probiotic and the stimulated resident fungi. Together, they could act in consortia to reduce the resources available for the pathogen, thereby negatively affecting pathogen density. This mode of pathogen resistance by microbial resource competition networks was recently observed in bacterial communities (Wei *et al.*, 2015), and our work extends this mechanism to include fungal communities.

It has been reported that plant-associated bacteria (e.g. *Pseudomonas*) and fungi (e.g. *Trichoderma*) can produce or release a variety of compounds that activate the immunity of plants to prevent pathogen infections (Harman *et al.*, 2004; Pieterse *et al.*, 2014; Salwan *et al.*, 2022). Therefore, we have also studied the effects of *Tg* and *Humicola* on the induced systemic resistance (ISR) of banana plant. We noticed that *Tg* and *Humicola* could significantly increase JA and SA contents in banana plants. Interestingly, we observed that the defense system in banana plants is more responsive to the inoculation of the combination of *Tg* and *Humicola*, suggesting that these two fungi could cooperatively induce plant resistance via the JA and SA signaling pathways. In addition, the combination of *Tg* and *Humicola* also conferred a greater activation effect on the ISR-related enzyme activities (e.g. CHT, POD, PAL, LOX, and PPO) in banana plants than single fungal species. These findings are in accordance with previous studies reported that plant hormones-induced pathways always accompanied by producing CHT and oxidative enzymes (e.g., POD, PAL, LOX, and PPO), and increased PAL and POD activities could furtherly enhance the production of phenolics and lignification to prevent pathogen invasion (Christopoulos & Tsantili, 2015; Mohamed *et al.*, 2020; Li *et al.*, 2021).

Indeed, we demonstrate that the cooperative interactions with the resident microbiome may have a larger effect on disease suppression than direct antagonistic action of inoculated biocontrol agents. This provides both mechanistic insights and a direct guide for targeted microbiome engineering to defend plants from plant pathogens.

## Conclusions

Our results show that application of the fungal probiotic agent *Tg* resulted in a reshaping of the soil fungal community, including the recruitment of beneficial fungal species that have the potential to protect plants together with *Tg* against the pathogen infection. These results offer new perspectives toward

the development of effective and sustainable solutions to improve crop protection. Fungal plant pathogens pose an ever-increasing threat for agriculture (Strange & Scott, 2005), and recent evidence suggests that the soil microbiome plays an essential role in controlling the onset of disease (Mendes *et al.*, 2011; Kwak *et al.*, 2018). Understanding the mechanisms that drive community assembly and the development of pathogen-suppressive soils is prerequisite to developing systematic approaches to harnessing beneficial microbiome for crop protection. While previous studies have highlighted the role of bacterial communities in the development of suppressive capabilities of soil, we demonstrate here that impacts on fungal community composition and specific interactions within the fungal community can be important drivers of disease suppression and plant health.

## Acknowledgements

This research was supported by the National Natural Science Foundation of China (32102475), the Fundamental Research Funds for the Central Universities (XUEKEN2022004, KYQN2022020, and KYQN2022025), the Guidance Foundation, the Sanya Institute of Nanjing Agricultural University (NAUSY-MS10), the Hainan Provincial Natural Science Foundation of China (322MS092), the China Postdoctoral Science Foundation (2021TQ0156 and 2021M691613), the Achievement Transformation Fund project of Hainan Research Institute of Nanjing Agricultural University (NAUSY-CG-ZD-01), and the Priority Academic Program Development of the Jiangsu Higher Education Institutions (PAPD).

## Competing interests

None declared.

## Author contributions

CT, RL, ZW, and SL performed all experiments. RL, CT, GAK, and QS designed the study and wrote the majority of the manuscript. CT analyzed the data. WX, NL, XD, ZS, NZ, and SG participated in the design of the study, provided comments, and edited the manuscript.

## ORCID

- Xuhui Deng  <https://orcid.org/0000-0002-5680-8100>
- Stefan Geisen  <https://orcid.org/0000-0003-0734-727X>
- George A. Kowalchuk  <https://orcid.org/0000-0003-3866-0832>
- Rong Li  <https://orcid.org/0000-0002-2599-5476>
- Qirong Shen  <https://orcid.org/0000-0002-5662-9620>
- Zongzhan Shen  <https://orcid.org/0000-0002-1886-0952>
- Chengyuan Tao  <https://orcid.org/0000-0002-4199-211X>
- Zhe Wang  <https://orcid.org/0000-0001-6106-2625>
- Wu Xiong  <https://orcid.org/0000-0001-5766-7998>
- Nan Zhang  <https://orcid.org/0000-0001-8444-7456>

## Data availability

All raw sequence data are available in NCBI Sequence Read Archive (SRA) database under the accession no. SRP286351. All codes used in this study are available from the corresponding author on request.

## References

Anderson MJ. 2001. A new method for non-parametric multivariate analysis of variance. *Austral Ecology* 26: 32–46.

Bai Y, Muller DB, Srinivas G, Garrido-Oter R, Potthoff E, Rott M, Dombrowski N, Munch PC, Spaepen S, Remus-Emsermann M *et al.* 2015. Functional overlap of the *Arabidopsis* leaf and root microbiota. *Nature* 528: 364–369.

Berendsen RL, Pieterse CM, Bakker PA. 2012. The rhizosphere microbiome and plant health. *Trends in Plant Science* 17: 478–486.

Caporaso JG, Kuczynski J, Stombaugh J, Bittinger K, Bushman FD, Costello EK, Fierer N, Peña AG, Goodrich JK, Gordon JI *et al.* 2010. QIIME allows analysis of high-throughput community sequencing data. *Nature Methods* 7: 335–336.

Caporaso JG, Lauber CL, Walters WA, Berg-Lyons D, Lozupone CA, Turnbaugh PJ, Fierer N, Knight R. 2011. Global patterns of 16S rRNA diversity at a depth of millions of sequences per sample. *Proceedings of the National Academy of Sciences, USA* 108: 4516–4522.

Chen L, Jiang Y, Liang C, Luo Y, Xu Q, Han C, Zhao Q, Sun B. 2019. Competitive interaction with keystone taxa induced negative priming under biochar amendments. *Microbiome* 7: 77.

Christopoulos MV, Tsantili E. 2015. Participation of phenylalanine ammonia-lyase (PAL) in increased phenolic compounds in fresh cold stressed walnut (*Juglans regia* L.) kernels. *Postharvest Biology and Technology* 104: 17–25.

Costello EK, Stagaman K, Dethlefsen L, Bohannan BJM, Relman DA. 2012. The application of ecological theory toward an understanding of the human microbiome. *Science* 336: 1255–1262.

De'ath G. 2002. Multivariate regression trees: a new technique for modeling species-environment relationships. *Ecology* 83: 1105–1117.

Duran P, Thiergart T, Garrido-Oter R, Agler M, Kemen E, Schulze-Lefert P, Hacquard S. 2018. Microbial interkingdom interactions in roots promote *Arabidopsis* survival. *Cell* 175: 973–983.

Edgar RC. 2010. Search and clustering orders of magnitude faster than BLAST. *Bioinformatics* 26: 2460–2461.

Edgar RC. 2013. UPARSE: highly accurate OTU sequences from microbial amplicon reads. *Nature Methods* 10: 996–998.

Elsas JD, Chiurazzi M, Mallon CA, Elhottova D, Křišťufek V, Salles JF. 2012. Microbial diversity determines the invasion of soil by a bacterial pathogen. *Proceedings of the National Academy of Sciences, USA* 109: 1159–1164.

Faith DP. 1992. Conservation evaluation and phylogenetic diversity. *Biological Conservation* 61: 1–10.

Fierer N, Jackson JA, Vilgalys R, Jackson RB. 2005. Assessment of soil microbial community structure by use of taxon-specific quantitative PCR assays. *Applied and Environmental Microbiology* 71: 4117–4120.

Fu L, Penton CR, Ruan Y, Shen Z, Xue C, Li R, Shen Q. 2017. Inducing the rhizosphere microbiome by biofertilizer application to suppress banana Fusarium wilt disease. *Soil Biology and Biochemistry* 104: 39–48.

Grice EA, Segre JA. 2011. The skin microbiome. *Nature Reviews Microbiology* 9: 244–253.

Harman GE, Howell CR, Viterbo A, Chet I, Lorito M. 2004. *Trichoderma* species—opportunistic, avirulent plant symbionts. *Nature Reviews Microbiology* 2: 43–56.

Hu J, Wei Z, Friman VP, Gu SH, Wang XF, Eisenhauer N, Yang TJ, Ma J, Shen QR, Xu YC *et al.* 2016. Probiotic diversity enhances rhizosphere microbiome function and plant disease suppression. *MBio* 7: e01790-16.

Hu J, Yang T, Friman VP, Kowalchuk GA, Hautier Y, Li M, Wei Z, Xu Y, Shen Q, Jousset A. 2021. Introduction of probiotic bacterial consortia promotes plant growth via impacts on the resident rhizosphere microbiome. *Proceedings of the Royal Society B: Biological Sciences* 288: 20211396.

Jambhulkar PP, Sharma P, Manokaran R, Lakshman DK, Rokadia P, Jambhulkar N. 2018. Assessing synergism of combined applications of *Trichoderma harzianum* and *Pseudomonas fluorescens* to control blast and bacterial leaf blight of rice. *European Journal of Plant Pathology* 152: 747–757.

Jeger MJ, Eden-Green S, Thresh JM, Johanson A, Waller JM, Brown AE. 1995. Banana diseases. In: Gowen S, ed. *Bananas and plantains*. Dordrecht, the Netherlands: Springer, 317–381.

Ji P, Wilson M. 2002. Assessment of the importance of similarity in carbon source utilization profiles between the biological control agent and the pathogen in biological control of bacterial speck of tomato. *Applied and Environmental Microbiology* 68: 4383–4389.

Jiang TT, Shao TY, Ang WXG, Kinder JM, Turner LH, Pham G, Whitt J, Alenghat T, Way SS. 2017. Commensal fungi recapitulate the protective benefits of intestinal bacteria. *Cell Host & Microbe* 22: 809–816.

Jiao S, Chen W, Wang J, Du N, Li Q, Wei G. 2018. Soil microbiomes with distinct assemblies through vertical soil profiles drive the cycling of multiple nutrients in reforested ecosystems. *Microbiome* 6: 146.

Jiménez-Fernández D, Montes-Borrego M, Navas-Cortés JA, Jiménez-Díaz RM, Landa BB. 2010. Identification and quantification of *Fusarium oxysporum* in planta and soil by means of an improved specific and quantitative PCR assay. *Applied Soil Ecology* 46: 372–382.

Jin T, Wang Y, Huang Y, Xu J, Zhang P, Wang N, Liu X, Chu H, Liu G, Jiang H *et al.* 2017. Taxonomic structure and functional association of foxtail millet root microbiome. *Gigascience* 6: 1–12.

Kandula DRW, Jones EE, Stewart A, McLean KL, Hampton JG. 2015. *Trichoderma* species for biocontrol of soil-borne plant pathogens of pasture species. *Biocontrol Science and Technology* 25: 1052–1069.

Kogo T, Yoshida Y, Koganei K, Matsumoto H, Watanabe T, Ogihara J, Kasumi T. 2017. Production of rice straw hydrolysis enzymes by the fungi *Trichoderma reesei* and *Humicola insolens* using rice straw as a carbon source. *Bioresource Technology* 233: 67–73.

Komada H. 1975. Development of a selective medium for quantitative isolation of *Fusarium oxysporum* from natural soil. *Review of Plant Protection Research* 8: 114–124.

Kozich JJ, Westcott SL, Baxter NT, Highlander SK, Schloss PD. 2013. Development of a dual-index sequencing strategy and curation pipeline for analyzing amplicon sequence data on the MiSeq Illumina sequencing platform. *Applied and Environmental Microbiology* 79: 5112–5120.

Kwak M-J, Kong HG, Choi K, Kwon S-K, Song JY, Lee J, Lee PA, Choi SY, Seo M, Lee HJ *et al.* 2018. Rhizosphere microbiome structure alters to enable wilt resistance in tomato. *Nature Biotechnology* 36: 1100–1109.

Lee SM, Kong HG, Song GC, Ryu CM. 2021. Disruption of Firmicutes and Actinobacteria abundance in tomato rhizosphere causes the incidence of bacterial wilt disease. *The ISME Journal* 15: 330–347.

Leśmanczyk G, Sadowski CK. 2002. Fungal communities and health status of roots of winter wheat cultivated after oats and oats mixed with other crops. *BioControl* 47: 349–361.

Letunic I, Bork P. 2019. Interactive Tree Of Life (iTOL) v4: recent updates and new developments. *Nucleic Acids Research* 47: W256–W259.

Li J, Philp J, Li J, Wei Y, Li H, Yang K, Ryder M, Toh R, Zhou Y, Denton MD *et al.* 2020. *Trichoderma harzianum* inoculation reduces the incidence of clubroot disease in Chinese cabbage by regulating the rhizosphere microbial community. *Microorganisms* 8: 1325.

Li M, Wei Z, Wang J, Jousset A, Friman VP, Xu Y, Shen Q, Pommier T. 2019. Facilitation promotes invasions in plant-associated microbial communities. *Ecology Letters* 22: 149–158.

Li Z, Bai X, Jiao S, Li Y, Li P, Yang Y, Zhang H, Wei G. 2021. A simplified synthetic community rescues *Astragalus mongolicus* from root rot disease by activating plant-induced systemic resistance. *Microbiome* 9: 217.

Matrood AAA, Khrieba MI, Okon OG. 2020. Synergistic interaction of *Glomus mosseae* T. and *Trichoderma harzianum* R. in the induction of systemic resistance of *Cucumis sativus* L. to *Alternaria Alternata* (Fr.) K. *Plant Science Today* 7: 101–108.

Mendes R, Kruijt M, de Bruijn I, Dekkers E, van der Voort M, Schneider JH, Piceno YM, DeSantis TZ, Andersen GL, Bakker PA *et al.* 2011. Deciphering the rhizosphere microbiome for disease-suppressive bacteria. *Science* 332: 1097–1100.

Mohamed BFF, Sallam NMA, Alamri SAM, Abo-Elyousr KAM, Mostafa YS, Hashem M. 2020. Approving the biocontrol method of potato wilt caused by *Ralstonia solanacearum* (Smith) using *Enterobacter cloacae* PS14 and *Trichoderma asperellum* T34. *Egyptian Journal of Biological Pest Control* 30: 1–13.

Mueller UG, Sachse JL. 2015. Engineering microbiomes to improve plant and animal health. *Trends in Microbiology* 23: 606–617.

Oksanen J, Blanchet FG, Kindt R, Legendre P, Minchin PR, O'Hara RB, Simpson GL, Solymos P, Stevens MHH, Wagner H. 2012. *VEGAN: community ecology package*. R Package v.2.0-4. [WWW document] URL <https://CRAN.R-project.org/package=vegan> [accessed 19 March 2017].

Org E, Blum Y, Kasela S, Mehrabian M, Kuusisto J, Kangas AJ, Soininen P, Wang Z, Ala-Korpela M, Hazen SL *et al.* 2017. Relationships between gut microbiota, plasma metabolites, and metabolic syndrome traits in the METSIM cohort. *Genome Biology* 18: 70.

Pierce EC, Morin M, Little JC, Liu RB, Tannous J, Keller NP, Pogliano K, Wolfe BE, Sanchez LM, Dutton RJ. 2021. Bacterial-fungal interactions revealed by genome-wide analysis of bacterial mutant fitness. *Nature Microbiology* 6: 87–102.

Pieterse CM, Zamioudis C, Berendsen RL, Weller DM, Van Wees SC, Bakker PA. 2014. Induced systemic resistance by beneficial microbes. *Annual Review of Phytopathology* 52: 347–375.

Qiu M, Zhang R, Xue C, Zhang S, Li S, Zhang N, Shen Q. 2012. Application of bio-organic fertilizer can control Fusarium wilt of cucumber plants by regulating microbial community of rhizosphere soil. *Biology and Fertility of Soils* 48: 807–816.

Raaijmakers JM, Mazzola M. 2016. Soil immune responses. *Science* 352: 1392–1393.

Romanuk TN, Zhou Y, Brose U, Berlow EL, Williams RJ, Martinez ND. 2009. Predicting invasion success in complex ecological networks. *Philosophical Transactions of the Royal Society B: Biological Sciences* 364: 1743–1754.

Saleem M, Hu J, Jousset A. 2019. More than the sum of its parts: microbiome biodiversity as a driver of plant growth and soil health. *Annual Review of Ecology, Evolution, and Systematics* 50: 145–168.

Salwan R, Sharma A, Kaur R, Sharma R, Sharma V. 2022. The riddles of *Trichoderma* induced plant immunity. *Biological Control* 174: 105037.

Schloss PD, Westcott SL, Ryabin T, Hall JR, Hartmann M, Hollister EB, Lesniewski RA, Oakley BB, Parks DH, Robinson CJ *et al.* 2009. Introducing mothur: open-source, platform-independent, community-supported software for describing and comparing microbial communities. *Applied and Environmental Microbiology* 75: 7537–7541.

Schoch CL, Seifert KA, Huhndorf S, Robert V, Spouge JL, Levesque CA, Chen W, Fungal Barcoding Consortium, Fungal Barcoding Consortium Author List. 2012. Nuclear ribosomal internal transcribed spacer (ITS) region as a universal DNA barcode marker for Fungi. *Proceedings of the National Academy of Sciences, USA* 109: 6241–6246.

Segata N, Izard J, Waldron L, Gevers D, Miropolsky L, Garrett WS, Huttenhower C. 2011. Metagenomic biomarker discovery and explanation. *Genome Biology* 12: R60.

Sessitsch A, Pfaffenbichler N, Mitter B. 2019. Microbiome applications from lab to field: facing complexity. *Trends in Plant Science* 24: 194–198.

Shen Z, Xue C, Penton CR, Thomashow LS, Zhang N, Wang B, Ruan Y, Li R, Shen Q. 2019. Suppression of banana Panama disease induced by soil microbiome reconstruction through an integrated agricultural strategy. *Soil Biology and Biochemistry* 128: 164–174.

Shin SC, Kim SH, You H, Kim B, Kim AC, Lee KA, Yoon JH, Ryu JH, Lee WJ. 2011. Drosophila microbiome modulates host developmental and metabolic homeostasis via insulin signaling. *Science* 334: 670–674.

Singh A, Lasek-Nesselquist E, Chaturvedi V, Chaturvedi S. 2018. *Trichoderma polyporum* selectively inhibits white-nose syndrome fungal pathogen *Pseudogymnoascus destructans* amidst soil microbes. *Microbiome* 6: 139–149.

Singh MP. 2009. Application of biolog FF MicroPlate for substrate utilization and metabolite profiling of closely related fungi. *Journal of Microbiological Methods* 77: 102–108.

Strange RN, Scott PR. 2005. Plant disease: a threat to global food security. *Annual Review of Phytopathology* 43: 83–116.

Sun X, Xu Z, Xie J, Hesselberg-Thomsen V, Tan T, Zheng D, Strube ML, Dragos A, Shen Q, Zhang R *et al.* 2021. *Bacillus velezensis* stimulates resident rhizosphere *Pseudomonas stutzeri* for plant health through metabolic interactions. *The ISME Journal* 16: 774–787.

Tao C, Li R, Xiong W, Shen Z, Liu S, Wang B, Ruan Y, Geisen S, Shen Q, Kowalchuk GA. 2020. Bio-organic fertilizers stimulate indigenous soil *Pseudomonas* populations to enhance plant disease suppression. *Microbiome* 8: 137.

Toju H, Peay KG, Yamamichi M, Narisawa K, Hiruma K, Naito K, Fukuda S, Ushio M, Nakaoka S, Onoda Y *et al.* 2018. Core microbiomes for sustainable agroecosystems. *Nature Plants* 4: 247–257.

Wagg C, Schlaepi K, Banerjee S, Kuramae EE, van der Heijden MGA. 2019. Fungal-bacterial diversity and microbiome complexity predict ecosystem functioning. *Nature Communications* 10: 4841.

Wang B, Yuan J, Zhang J, Shen Z, Zhang M, Li R, Ruan Y, Shen Q. 2013. Effects of novel bioorganic fertilizer produced by *Bacillus amyloliquefaciens* W19 on antagonism of Fusarium wilt of banana. *Biology and Fertility of Soils* 49: 435–446.

Wang Q, Garrity GM, Tiedje JM, Cole JR. 2007. Naive Bayesian classifier for rapid assignment of rRNA sequences into the new bacterial taxonomy. *Applied and Environmental Microbiology* 73: 5261–5267.

Wei Z, Yang T, Friman VP, Xu Y, Shen Q, Jousset A. 2015. Trophic network architecture of root-associated bacterial communities determines pathogen invasion and plant health. *Nature Communications* 6: 8413.

Xiong W, Guo S, Jousset A, Zhao Q, Wu H, Li R, Kowalchuk GA, Shen Q. 2017. Bio-fertilizer application induces soil suppressiveness against Fusarium wilt disease by reshaping the soil microbiome. *Soil Biology and Biochemistry* 114: 238–247.

Yang T, Wei Z, Friman VP, Xu Y, Shen Q, Kowalchuk GA, Jousset A. 2017. Resource availability modulates biodiversity-invasion relationships by altering competitive interactions. *Environmental Microbiology* 19: 2984–2991.

Yuan J, Wen T, Zhang H, Zhao M, Penton CR, Thomashow LS, Shen Q. 2020. Predicting disease occurrence with high accuracy based on soil macroecological patterns of Fusarium wilt. *The ISME Journal* 14: 2936–2950.

Zhang J, Miao Y, Rahimi MJ, Zhu H, Steindorff A, Schiessler S, Cai F, Pang G, Chenthama K, Xu Y *et al.* 2019. Guttation capsules containing hydrogen peroxide: an evolutionarily conserved NADPH oxidase gains a role in wars between related fungi. *Environmental Microbiology* 21: 2644–2658.

Zhang Y, Wang X, Pang G, Cai F, Zhang J, Shen Z, Li R, Shen Q. 2019. Two-step genomic sequence comparison strategy to design *Trichoderma* strain-specific primers for quantitative PCR. *AMB Express* 9: 179.

Zhang Y, Xu J, Riera N, Jin T, Li J, Wang N. 2017. Huanglongbing impairs the rhizosphere-to-rhizoplane enrichment process of the citrus root-associated microbiome. *Microbiome* 5: 97.

Zhao X, Song L, Jiang L, Zhu Y, Gao Q, Wang D, Xie J, Lv M, Liu P, Li M. 2020. The integration of transcriptomic and transgenic analyses reveals the involvement of the SA response pathway in the defense of chrysanthemum against the necrotrophic fungus *Alternaria* sp. *Hortic Research* 7: 80.

Zhou Y, Yang L, Wang J, Guo L, Huang J. 2021. Synergistic effect between *Trichoderma virens* and *Bacillus velezensis* on the control of tomato bacterial wilt disease. *Horticulturae* 7: 439.

## Supporting Information

Additional Supporting Information may be found online in the Supporting Information section at the end of the article.

**Fig. S1** Banana wilt disease incidence and plant biomass in each crop season.

**Fig. S2** Abundance of total fungi in different fertilization treatments.

**Fig. S3** Evolutionary relationships of *Trichoderma* isolates and *Trichoderma* operational taxonomic units (OTUs) with *Tg*.

**Fig. S4** Linear regression relationships between fungal abundance with banana plant disease and biomass.

**Fig. S5** Fungal phylogenetic diversity (Faith's PD) indices and multiple regression tree (MRT) analysis.

**Fig. S6** Taxonomic dendrogram of the core fungal microbiome influenced by fertilization regimes.

**Fig. S7** Soil microbial carbon metabolic activities.

**Fig. S8** Fungal co-occurrence networks and module-metabolic associations.

**Fig. S9** Linear regression relationships between fungal diversity with banana plant disease and biomass.

**Fig. S10** Random forest model regress fungal microbiome against banana plant disease and biomass.

**Fig. S11** Linear regression relationships between fungal operational taxonomic units (OTUs) with banana plant disease and biomass.

**Fig. S12** Effects of different concentrations of *Tg* on fungal community diversity and composition.

**Fig. S13** Effects of fertilization treatments on soil culturable fungal microbiome.

**Fig. S14** Interactions of *Tg* and FOC with fungal isolates.

**Fig. S15** Effects of fungal consortia *Tg-Humicola* on FOC population densities and hypha growth.

**Tables S1** The primers required for qPCR.

**Tables S2** The reaction mixture compositions of qPCR.

**Tables S3** The reaction conditions of qPCR.

**Table S4** PERMANOVA results of fungal community composition at the operational taxonomic unit (OTU) level.

**Table S5** Mantel test between fungal community composition with banana plant disease and biomass.

**Table S6** Linear models (LMs) for relationships of microbial indicators with banana plant disease and biomass.

**Table S7** *Tg* and FOC-suppressing ability of fungal isolates isolated from sterilized organic fertilizer (SOF) and SOF + *Tg* soils.

Please note: Wiley is not responsible for the content or functionality of any Supporting Information supplied by the authors. Any queries (other than missing material) should be directed to the *New Phytologist* Central Office.